Thermal fluctuations and x-ray scattering from free-standing smectic-*A* films

L. V. Mirantsev
Institute of the Problems of Mechanical Engineering, Academy of Sciences of Russia, St. Petersburg 199178, Russia
(Received 7 February 2000)

The present paper is devoted to theoretical investigation of thermal fluctuations and correlations between them in free-standing smectic-*A* films (FSS*A*F's) formed of liquid crystal compounds with bulk smectic-*A*–isotropic (Sm*A*-*I*) and Sm*A*–nematic (Sm*A*-*N*) phase transitions, as well as small angle x-ray scattering from these FSS*A*F's. The study took into account the dependence of the bending elastic constant *K* and the smectic layer compressibility *B* on the distance from the boundary free surfaces of the films. The results of calculation are compared with those obtained in the framework of the Holyst model [Phys. Rev. Lett. **65**, 2153 (1990); Phys. Rev. A. **44**, 3692 (1991)] for spatially uniform FSS*A*F's. It has been found that, well below the temperature at which the smectic order in the bulk liquid crystal disappears, taking into account the profiles of the elastic moduli *K* and *B* does not produce noticeable differences from this model. However, at maximum temperatures of existence of FSS*A*F's, our results are considerably different from the predictions of the Holyst model. The results obtained are applied to calculation of specular and diffuse x-ray reflectivities of FSS*A*F's in the whole temperature interval of their existence. Displacement of the molecular centers within the film layers along those normal to them and the deviation of the local orientational order in FSS*A*F's from the ideal are also taken into account. The results of calculation are in agreement with experiments on the small angle x-ray scattering from FSS*A*F's.

PACS number(s): 61.30.Cz, 64.70.Md

I. INTRODUCTION

A unique property of smectic liquid crystals is the ability to form free-standing films, and during last 10–20 years these films are the objects of intensive experimental [1–28] and theoretical [29–39] investigations. The surface area of free-standing smectic films (FSSF's), which can be considered as stacks of smectic layers with two boundary free surfaces, can be as large as $\sim \mathrm{cm}^2$ [1], and their thickness can be varied from thousands of molecular layers down to two and even one smectic layer [2,3]. Hence, varying the film thickness, one can study the crossover from three-dimensional (3D) to 2D behavior. In addition, the combination of the surface-induced ordering and finite-size effects in FSSF's gives rise to the appearance of phenomena that are not observed in bulk liquid crystal (LC) samples. First, the temperatures of phase transitions in FSSFs can be significantly different from those in bulk LC samples [4–10], and in sufficiently thin films the first order phase transitions become the second order ones. Second, in FSSF's of some LC's one can observe smectic phases which are not observed in the bulk samples of the same LC compounds [11–13]. Finally, remarkable phenomena, namely, layer-thinning transitions, have been recently discovered in free-standing smectic-*A* films (FSS*A*F's) of certain LC materials [14–18]. These films do not rupture upon heating above temperature of the bulk smectic-*A*–isotropic (Sm*A*-*I*) or smectic-*A*–nematic (Sm*A*-*N*) phase transition, but undergo a series of thinning transitions. Via these transitions the film with initial thickness of several tens of smectic layers can thin step by step to two layers, and the temperature of existence of the final two-layer film can be about 10–20 K higher than the bulk Sm*A*-*I* or Sm*A*-*N* transition temperatures.

A most complete set of information on structure of FSSF's can be obtained from experiments on x-ray reflectivity. These experiments provide us with information on both equilibrium properties of the films and thermal fluctuations in them. Measuring a specular reflectivity, one can determine [11–13,22–24] a number of the film layers, the layer spacing, the local layer structure as well as the thermal fluctuation profile [18,24,35,26–28]. On the other hand, studying the x-ray diffuse scattering [26–28] reveals the correlations between the fluctuations in the different film layers. However, this information cannot be extracted from the experimental data without an adequate theoretical model for both equilibrium structure of the FSSF and thermal fluctuations in the film. A simple discrete model for the thermal fluctuations in FSS*A*F's, which takes into account not only the bending and compression of the smectic layers, but also the surface tension of the film, has been proposed by Holyst [31,32]. Later, the continuous versions of the Holyst's model have been developed in Refs. [33] and [34]. The model allows us to easily calculate the smectic layer displacement fluctuation profile and the displacement-displacement correlations in the FSS*A*F, and the results of these calculations are in a very good agreement with data of experiments [26,27] on small angle specular and diffuse x-ray scattering from FSS*A*F's of some LC compounds.

However, the Holyst's model has two essential defects. The first defect is that in the framework of this model the FSS*A*F is assumed to be spatially homogeneous and characterized with only four physical parameters, namely, the number of the smectic layers *N*, the surface tension γ, and the elastic constants *K* and *B* for bending and compression of the smectic layers, respectively. The latter constants are assumed to be similar for all film layers and equal to those for the bulk Sm*A* phase. This assumption is physically justified only for FSS*A*F's studied at temperatures significantly lower than the bulk Sm*A*-*I* or Sm*A*-*N* transition temperatures. In this case the Sm*A* structure is well developed in whole volume of the

film, and both orientational and translational molecular ordering in internal film layers should be similar to those near the boundary free surfaces. Since the bending elastic constant K is proportional to s^2, and the smectic layer compressibility B is proportional to τ^2 [40,41], where s and τ are the orientational and translational order parameters, respectively, the elastic constants K and B should also be almost equal for all film layers. As said above, however, FSS*A*F's of some LCs can exist at temperatures much higher than the bulk Sm*A*-*I* or Sm*A*-*N* transition temperatures [14–18]. According to the microscopic model proposed in Refs. [35,36] and [39], which describes many features of behavior of the FSS*A*F's at these temperatures [42], well above the bulk Sm*A*-*I* or Sm*A*-*N* transition points the internal film layers can be significantly less ordered than the outermost ones. This theoretical result has been experimentally confirmed by experiments on x-ray scattering from FSS*A*F's of LC compound 4,4'-diheptyl-azoxybenzene (7AB) heated above the bulk Sm*A*-*N* transition temperature [18]. Thus in such films both the bending elastic constant K and the smectic layer compressibility B should decrease with distance from the boundary free surface and reach minimal values in the interior of the film. In the Holyst model [31,32] and its later versions [33,34] such profiles of the elastic constants K and B are not taken into account, and, consequently, above the bulk Sm*A*-*I* or Sm*A*-*N* transition temperatures these models should not give correct values of the smectic layer displacement fluctuations and correlations between them. Another essential defect of the Holyst's model is that the layered Sm*A* structure is considered as a set of equidistant planes, in which the molecular centers are disposed, and a temperature dependent displacement of the molecular centers within each smectic layer along the normal to it is completely ignored. In addition, all LC molecules in the film are assumed to be rigorously aligned parallel to the normal to the film layers, i.e., the orientational order in the film is assumed to be ''ideal.'' Thus, in the framework of the Holyst model, a temperature dependent ''local disorder'' within smectic layers is completely neglected, and deviation of the one-dimensional positional order in the film from ideal is assumed to be related only to hydrodynamic displacements of the smectic layers from their equilibrium positions.

Because of the above mentioned defects, the Holyst model predicts the specular and diffuse x-ray reflectivities of FSS*A*F to be almost completely temperature independent, that is, in contradiction with experiments [18] on the small angle x-ray scattering from FSS*A*F's of the LC compound 7AB. In order to fit the data of these experiments to results of calculations performed in the framework of the Holyst model, the mean square amplitude σ_{tot}^2 of the thermal fluctuations in the film is assumed to be composed of two parts, namely,

$$\sigma_{tot}^2 = \sigma^2 + \sigma_{loc}^2 , \tag{1}$$

where σ^2 is a mean square amplitude of the smectic layer displacement fluctuations given by the model [31,32] or its continuous modifications [33,34], and σ_{loc}^2 is the mean square amplitude of fluctuations related to the local disorder within the smectic layers. The latter value is introduced *ad hoc*, and a satisfactory fit of data on the specular x-ray reflectivity of FSS*A*F's at temperatures well above the bulk Sm*A*-*N* transition point can be achieved only when the local disorder is assumed to be minimal near the boundary free surfaces of the film and maximal in its interior layers. At the same time, however, the elastic constants K and B, which, as said above, must be determined by the orientational and positional order within the smectic layers, are assumed to be similar for all film layers. It is clear that such description of the thermal fluctuations in FSS*A*F's is essentially contradictory, and in Ref. [18] it has been noted a necessity to modify the Holyst model and take into account simultaneously a spatial inhomogeneity of the film and the local disorder within its smectic layers.

In the present paper we offer a simple generalization of the Holyst discrete model [31,32] which takes into account both the bending elastic constant K and smectic layer compressibility B profiles. These profiles are determined from microscopic model for FSS*A*F proposed in Refs. [35,36] and [39]. For FSS*A*F formed of compounds exhibiting both Sm*A*-*I* and Sm*A*-*N* phase transitions, the smectic layer displacement fluctuation profiles and the displacement-displacement correlations have been calculated. The results of calculations are compared with those obtained in the framework of the Holyst model. It has been found that below the bulk Sm*A*-*I* or Sm*A*-*N* transition temperatures our results is quite similar to those given by this model. However, well above the bulk phase transition temperatures, the results of our calculations are significantly different from predictions obtained in the framework of the Holyst model. Using these results and the results of the microscopic model [35,36,39] for FSS*A*F's, which takes into account the displacement of the molecular centers within smectic layers along the normal to them and the deviation of the local orientational order in the film layers from ideal, we have also calculated the specular and diffuse x-ray reflectivities of FSS*A*F's of given thickness in whole temperature interval of their existence. The results of calculations are in agreement with data of experiments [18,26–28] on the small x-ray scattering from FSS*A*F's.

We start in the next section with a description of the smectic layer displacement fluctuations and correlations between them in FSS*A*F with taking into account the bending elastic constant K and the smectic layer compressibility B profiles obtained from the microscopic model [35,36,39] for FSS*A*F's. In Sec. III the results of this model and those obtained in Sec. II are used in calculations of the specular and diffuse x-ray reflectivities of FSS*A*F. Section IV presents the results of numerical calculations of the thermal fluctuations and correlations between them in FSS*A*F, as well as the specular and diffuse x-ray reflectivities of the free-standing Sm*A* films, followed by a discussion.

II. DESCRIPTION OF SMECTIC LAYER DISPLACEMENT FLUCTUATIONS IN FSS*A*F

Let us consider the N layer FSS*A*F. In this film the smectic layer displacements $u_n(x,y)$ from equilibrium positions $z_n^{(0)} = nd$ along the z-axis normal to the film layers, where n is the layer index and d is the smectic layer spacing, give rise to the free energy excess F consisting of surface F_S and bulk F_B contributions, respectively. According to the Holyst

model [31,32], the surface energy F_S, which is associated with an increase of the surface area of the two free surfaces, is given by

$$F_S=\frac{1}{2}\gamma\int[|\nabla_\perp u_1(\vec{R})|^2+|\nabla_\perp u_N(\vec{R})|^2]d\vec{R}, \tag{2}$$

where γ is the surface tension of the free surface of FSS*A*F, $\vec{R}$ is the radius-vector in the plane of the film ($R^2=x^2+y^2$), $\nabla_\perp$ is the projection of the $\vec{\nabla}$ operator on the (x,y) plane. As for the bulk contribution F_B to the free energy excess F, it consists of two parts which are associated with bending and compression of the smectic layers, respectively. If an elastic constant for bending of the nth smectic layer is denoted as K_n, and B_n is the compressibility of this layer, then, by analogy with the discrete Holyst model, the energy F_B can be written as

$$F_B=\frac{1}{2}\sum_{n=1}^{N}K_n d\int[\Delta_\perp u_n(\vec{R})]^2 d\vec{R}+\frac{1}{2}\sum_{n=1}^{N-1}\left(\frac{B_n+B_{n+1}}{2d}\right)\int[u_{n+1}(\vec{R})-u_n(\vec{R})]^2 d\vec{R}, \tag{3}$$

where $\Delta_\perp$ is the two-dimensional Laplacian in the (x,y) plane. Adding F_S and F_B, one can obtain the following expression for the total free energy excess F of FSS*A*F associated with the film layer displacement fluctuations:

$$F=\frac{1}{2}\int\left\{\sum_{n=1}^{N-1}\left(\frac{B_n+B_{n+1}}{2d}\right)[u_{n+1}(\vec{R})-u_n(\vec{R})]^2+\sum_{n=1}^{N}K_n d[\Delta_\perp u_n(\vec{R})]^2+\gamma\left|\nabla_\perp u_1(\vec{R})\right|^2+\gamma\left|\nabla_\perp u_N(\vec{R})\right|^2\right\}d\vec{R}. \tag{4}$$

It is easily seen that, for spatially uniform FSS*A*F, when the elastic constants K_n and B_n are similar for all film layers and equal to K and B, respectively, expression (4) for the total free energy excess F of FSS*A*F is completely similar to analogous expression proposed by Holyst (Eq. (3.2) in Ref. [32]). Then using, as in Refs. [31] and [32], the Fourier transformation

$$u_n(\vec{R})=(2\pi)^{-2}\int u_n(\vec{q}_\perp)\exp(i\vec{q}_\perp\cdot\vec{R})d\vec{q}_\perp, \tag{5}$$

we can rewrite the free energy F in the following compact form:

$$F=\frac{1}{2}\sum_{k,n=1}^{N}\int u_k(\vec{q}_\perp)M_{kn}u_n(-\vec{q}_\perp)d\vec{q}_\perp, \tag{6}$$

where M_{kn} are the elements of symmetrical ribbonlike matrix. The nonzero elements of this matrix are determined as

$$M_{11}=M_{NN}=\gamma q_\perp^2+K_1 d q_\perp^4+(B_1+B_2)/2d=b_1=b_N, \tag{7}$$

$$M_{nn}=K_n d q_\perp^4+(B_{n-1}+2B_n+B_{n+1})/2d=b_n,\quad n=2,\ N-1, \tag{8}$$

$$M_{n+1n}=M_{nn+1}=-(B_n+B_{n+1})/2d=c_n,\quad n=1,\ N-1. \tag{9}$$

Further, one can find the elements of inverse matrix and, using Eqs. (3.7) and (3.8) in Ref. [32], calculate the average film layer displacement fluctuations $\sigma_n=\langle u_n^2(0)\rangle^{1/2}$ and correlations $g_{k,n}(R)=\langle u_k(\vec{R})u_n(0)\rangle/(\sigma_k\sigma_n)$ between them.

As said above, the bending elastic constant K is proportional to s^2, and the smectic layer compressibility B is proportional to τ^2, where s and τ are the orientational and translational order parameters, respectively [40,41]. Using these relationships we can calculate the elastic constants K_n and B_n for the film layers via the microscopic model for FSS*A*F proposed in Refs. [35,36] and [39]. The model allows us to determine the local order parameters $s_n(T)$ and $\tau_n(T)$ for each FSS*A*F layer at any temperature T within the interval of its existence. In addition, for very thick films ($N\to\infty$), this model gives values of the order parameters s_n and τ_n for the interior film layers which completely coincide with results of well known McMillan theory [43] for bulk Sm*A* phase. So, if we know values of the elastic constants K and B for the bulk Sm*A* phase at a certain temperature T_0 [$K(T_0)\equiv K_0$, $B(T_0)\equiv B_0$] below the bulk Sm*A*-*I* or Sm*A*-*N* transition temperature, then, from the model [35,36,39], we can find values of the order parameters $s(T_0)\equiv s_0$ and $\tau(T_0)\equiv\tau_0$ at T_0, and, using relationships

$$K_n(T)=K_0[s_n(T)/s_0]^2,\quad B_n(T)=B_0[\tau_n(T)/\tau_0]^2, \tag{10}$$

determine values of the elastic constants K_n and B_n for each layer of FSS*A*F of given thickness at any temperature T within the interval of its existence.

III. X-RAY SCATTERING FROM FSS*A*F

The intensity of x-ray scattering from any system is proportional to the Fourier transform $S(\vec{Q})$ of the density-density correlation function given by Ref. [32]

$$S(\vec{Q})=\int d\vec{r}\int\langle\hat{\rho}(\vec{r})\hat{\rho}(\vec{r}')\rangle\exp[i\vec{Q}\cdot(\vec{r}-\vec{r}')]d\vec{r}', \tag{11}$$

where $\hat{\rho}(\vec{r})$ is the electron density operator, $\vec{Q}$ is the wave vector transfer related to the x-ray scattering from electrons of the system, and $\langle\cdots\rangle$ means average upon thermal fluctuations. The electron density operator $\hat{\rho}(\vec{r})$ for N-layer FSS*A*F can be, in turn, written as

$$\hat{\rho}(z)=\rho_0\sum_{k=1}^{N}\int_{-L/2\cos\vartheta}^{L/2\cos\vartheta}f_k(z-z',\vartheta)\times\Theta_k(z-z')\rho_e(z')dz'd\cos\vartheta. \tag{12}$$

Here ρ_0 is the molecular density in LC, $\rho_e(z')$ is the electron

density distribution in a single LC molecule, $f_k(z-z',\vartheta)$ is a one particle distribution function for the kth film layer, ϑ is a polar angle between the z axis and the long molecular one, L is the molecular length, and $\Theta_k(z-z')$ is a step function equal to 1 for $z_k^{(1)} \leqslant (z-z') \leqslant z_k^{(2)}$, and 0 for $(z-z')$ outside this interval.

In the equilibrium state, the coordinates $z_k^{(1)}$ and $z_k^{(2)}$, which determine positions of the lower and upper boundary planes of the kth film layer, can be written as $(k-1/2)d$ and $((k+1/2)d$, respectively. When the kth layer is displaced from its equilibrium position along the z axis by the value $u_k(\vec{r}_\perp)$, these coordinates become $(k-1/2)d+u_k(\vec{r}_\perp)$ and $(k+1/2)d+u_k(\vec{r}_\perp)$, respectively. Then Eq. (11) can be written in the form

$$S(\vec{Q}) = \rho_0^2 \int d\vec{r}_\perp \int \exp[i\vec{Q}_\perp(\vec{r}_\perp - \vec{r}'_\perp)]d\vec{r}'_\perp \Bigg\langle \sum_{k=1}^{N} \int_{(k-1/2)d+u_k(\vec{r}_\perp)}^{(k+1/2)d+u_k(\vec{r}_\perp)} f_k(z-z'',\vartheta) \times \exp[iQ_z(z-z'')]d(z-z'')d\cos\vartheta \int_{-L/2\cos\vartheta}^{L/2\cos\vartheta} \rho_e(z'')\exp(iQ_z z'')dz'' \times \sum_{n=1}^{N} \int_{(n-1/2)d+u_n(\vec{r}'_\perp)}^{(n+1/2)d+u_n(\vec{r}'_\perp)} f_n(z'-z''',\vartheta')\exp[iQ_z(z'-z''')]d(z'-z''')d\cos\vartheta' \times \int_{-L/2\cos\vartheta'}^{L/2\cos\vartheta'} \rho_e(z''')\exp(-iQ_z z''')dz''' \Bigg\rangle. \tag{13}$$

The calculations performed in Refs. [18] and [26–28] show that amplitudes σ_k of the layer displacement fluctuations in FSSAF's are usually much smaller than the smectic layer spacing d, and their profile should be smooth enough, i.e.,

$$|\sigma_{k+1}-\sigma_k|/(\sigma_{k+1}\sigma_k)^{1/2} \ll 1. \tag{14}$$

Then one can assume that both the local orientational and positional order within the film layers are not sensitive to such fluctuations, and hence the one particle distribution functions $f_k(z-z',\vartheta)$ should be the same as in the equilibrium state. In this case, it can be easily shown that Eq. (13) can be reduced to the following form:

$$S(\vec{Q}) = \rho_0^2 \int d\vec{r}_\perp \int \exp[i\vec{Q}_\perp\cdot(\vec{r}_\perp - \vec{r}'_\perp)]d\vec{r}'_\perp \sum_{k=1}^{N}\sum_{n=1}^{N} \langle \exp\{iQ_z(u_k(\vec{r}_\perp)-u_n(\vec{r}'_\perp))\}\rangle \exp[iQ_z(k-n)d] \times \int_{-d/2}^{+d/2} \exp(iQ_z z_1)dz_1 \int_0^1 f_k(z_1,\vartheta)S_{M1}(Q_z,\vartheta)d\cos\vartheta \times \int_{-d/2}^{+d/2} \exp(-iQ_z z_2)dz_2 \int_0^1 f_n(z_2,\vartheta')S_{M2}(Q_z,\vartheta')d\cos\vartheta', \tag{15}$$

where

$$S_{M1}(Q_z,\vartheta) = \int_{-L/2\cos\vartheta}^{L/2\cos\vartheta} \rho_e(z)\exp(iQ_z z)dz, \tag{16}$$

$$S_{M2}(Q_z,\vartheta) = \int_{-L/2\cos\vartheta}^{L/2\cos\vartheta} \rho_e(z)\exp(-iQ_z z)dz. \tag{17}$$

If it is also assumed that the electron density distribution $\rho_e(z')$ within a single LC molecule is symmetrical with respect to the molecular center, and the one particle distribution function is an even function of z, then

$$S(\vec{Q}) = 4\rho_0^2 \int d\vec{r}_\perp \int \exp[i\vec{Q}_\perp\cdot(\vec{r}_\perp - \vec{r}'_\perp)]d\vec{r}'_\perp \times \sum_{k=1}^{N}\sum_{n=1}^{N} \langle \exp\{iQ_z(u_k(\vec{r}_\perp)-u_n(\vec{r}'_\perp))\}\rangle \times \cos[(k-n)dQ_z]\eta_k(Q_z)\eta_n(Q_z), \tag{18}$$

where

$$\eta_k(Q_z) = \int_{-d/2}^{+d/2} \cos(Q_z z)dz \int_0^1 f_k(z,\vartheta)S_M(Q_z,\vartheta)d\cos\vartheta, \tag{19}$$

$$S_M(Q_z,\vartheta) = \int_0^{L/2\cos\vartheta} \rho_e(z)\cos(Q_z z)dz. \tag{20}$$

Finally, if we take into account that

$$\int d\vec{r}_\perp \int d\vec{r}'_\perp \exp[i\vec{Q}_\perp\cdot(\vec{r}_\perp - \vec{r}'_\perp)]\langle \exp\{iQ_z[u_k(\vec{r}_\perp) - u_n(\vec{r}'_\perp)]\}\rangle = S_0 \int d\vec{r}_\perp \exp(i\vec{Q}_\perp\cdot\vec{r}_\perp)\exp\{-(1/2) \times Q_z^2[\sigma_k^2+\sigma_n^2-2\langle u_k(\vec{r}_\perp)u_n(0)\rangle]\}, \tag{21}$$

where S_0 is the film surface area, then the expression for $S(\vec{Q})$ can be represented in the following compact form:

$$S(\vec{Q})=4\rho_0^2 S_0 \sum_{k=1}^{N}\sum_{n=1}^{N}\int d\vec{r}_\perp \exp(i\vec{Q}_\perp\cdot\vec{r}_\perp)\cos[(k-n)dQ_z] \times \eta_k(Q_z)\,\eta_n(Q_z)F_{kn}(Q_z)\times C_{kn}(Q_z,\vec{r}_\perp), \tag{22}$$

where

$$F_{kn}(Q_z)=\exp[-(1/2)Q_z^2(\sigma_k^2+\sigma_n^2)], \tag{23}$$

$$C_{kn}(Q_z,\vec{r}_\perp)=\exp[Q_z^2\langle u_k(\vec{r}_\perp)u_n(0)\rangle]. \tag{24}$$

Equation (22) differs from analogous expression for $S(\vec{Q})$ in Ref. [32] only with coefficients $\eta_k(Q_z)$. In the Holyst theory, in which both the orientational and positional order within the film layers are assumed to be ideal, these coefficients are simply equal to the molecular form factor (20) at $\vartheta=0$. The expressions for the one particle distribution functions $f_k(z-z',\vartheta)$ are brought in Refs. [35] and [36]. As for the form factor $S_M(Q_z,\vartheta)$, its form depends on a concrete model describing the electron density distribution within a single LC molecule. For example, when this distribution is assumed to be uniform, i.e., $\rho_e(z)=\rho_e$, the form factor $S_M(Q_z,\vartheta)$ is equal to

$$S_M(Q_z,\vartheta)=(\rho_e/Q_z)\sin(Q_zL\cos\vartheta/2). \tag{25}$$

If the LC molecules are assumed, as in Refs. [18] and [26–28], to be composed of a core with the electron density ρ_{core} amd two similar tails with density ρ_{tail}, then the form factor $S_M(Q_z,\vartheta)$ is given by

$$S_M(Q_z,\vartheta)=(\rho_{core}/Q_z)\{(\rho_{tail}/\rho_{core})\sin(Q_zL\cos\vartheta/2) -(\rho_{tail}/\rho_{core}-1) \times\sin[Q_z(L/2-d_{tail})\cos\vartheta]\}, \tag{26}$$

where d_{tail} is the molecular tail length.

For $\vec{Q}_\perp=\vec{0}$, Eq. (22) describes the specular x-ray reflection from FSS*A*F, and for $\vec{Q}_\perp\neq\vec{0}$, this equation describes the diffuse x-ray scattering from the film. However, it is convenient to consider both these cases separately. First, let us consider the specular reflection. It can be easily shown that in this case the factor $C_{kn}(Q_z,\vec{r}_\perp)$ in Eq. (22) can be with a good accuracy approximated by unit. Really, in Eq. (24) the correlator $\langle u_k(\vec{r}_\perp)u_n(0)\rangle$ in the exponent decays with growth of $|\vec{r}_\perp|$, and for LC with typical values of the elastic constants $K\sim10^{-6}$ dyn, $B\sim10^8$ dyn/cm^2, and for $|\vec{r}_\perp|$ larger than ~100 molecular diameters, i.e., ~400 A, its value does not exceed ~2 A^2 [32]. If we take, for example, the value of Q_z corresponding to the first Bragg maximum in the x-ray scattering pattern for FSS*A*F, i.e., $Q_z=2\pi/d$, then one can easily check that, for typical value of the smectic layer spacing $d\approx30$ A, the factor $C_{kn}(Q_z,\vec{r}_\perp)\approx1.09$. In actual experiments on the x-ray scattering from FSS*A*F's [18,26–28], their transverse size is of the order of ~1 cm, and, consequently, a dominant contribution to the reflected x-ray intensity is due to the values of $|\vec{r}_\perp|$ corresponding to $C_{kn}(Q_z,\vec{r}_\perp)$ much closer to unit than 1.09. Then, in case of the specular x-ray reflection from FSS*A*F, we can write

$$S(Q_z)\approx4\rho_0^2S_0^2\sum_{k=1}^{N}\sum_{n=1}^{N}\cos[(k-n)dQ_z] \times\eta_k(Q_z)\,\eta_n(Q_z)F_{kn}(Q_z). \tag{27}$$

Now let us turn to the x-ray diffuse scattering from FSS*A*F ($\vec{Q}_\perp\neq\vec{0}$). In this case we can expand Eq. (24) in series of $Q_z^2\langle u_k(\vec{r}_\perp)u_n(0)\rangle$ and restrict to first two terms. For the films of a macroscopic transverse size, the first term

$$\int\exp(i\vec{Q}_\perp\cdot\vec{r}_\perp)d\vec{r}_\perp=0,$$

and only the second term of the expansion gives a nonzero contribution to intensity of the diffuse x-ray scattering from FSS*A*F. Then we have

$$S(Q_z,\vec{Q}_\perp)\approx4\rho_0^2S_0\sum_{k=1}^{N}\sum_{n=1}^{N}\cos[(k-n)dQ_z] \times\eta_k(Q_z)\,\eta_n(Q_z)F_{kn}(Q_z)Q_z^2 \times\int\langle u_k(\vec{r}_\perp)u_n(0)\rangle\exp(i\vec{Q}_\perp\cdot\vec{r}_\perp)d\vec{r}_\perp. \tag{28}$$

Inserting expression (3.8) in Ref. [32] for correlator $\langle u_k(\vec{r}_\perp)u_n(0)\rangle$ into Eq. (28), and taking into account that

$$\frac{1}{(2\pi)^2}\int\exp[i(\vec{Q}_\perp-\vec{q}_\perp)\cdot\vec{r}_\perp]d\vec{r}_\perp=\delta(\vec{Q}_\perp-\vec{q}_\perp), \tag{29}$$

where $\delta(\vec{x})$ is the Dirac δ function, one can obtain

$$S(Q_z,\vec{Q}_\perp)\approx4\rho_0^2S_0k_BT\sum_{k=1}^{N}\sum_{n=1}^{N}\cos[(k-n)dQ_z] \times\eta_k(Q_z)\,\eta_n(Q_z) \times F_{kn}(Q_z)Q_z^2M_{kn}^{-1}(\vec{Q}_\perp). \tag{30}$$

Here $M_{kn}^{-1}(\vec{Q}_\perp)$ is the element of the matrix inverse to that brought in Sec. II, and k_B is the Boltzmann constant.

Equations (27) and (30) allow us to calculate the specular and diffuse x-ray reflectivities of N-layer FSS*A*F at any temperature T of its existence. The coefficients $\eta_k(Q_z)$ contain all information on the local orientational and positional molecular order within the film layers, the coefficients $F_{kn}(Q_z)$ determine dependence of the specular and diffuse x-ray reflectivities on average amplitudes σ_k of the smectic layer displacement fluctuations, and the matrix elements $M_{kn}^{-1}(\vec{Q}_\perp)$ determine dependences of thediffuse reflectivity on the correlations between the thermal fluctuations in FSS*A*F. It should be also noted that amplitudes σ_k of these fluctuations and the matrix elements $M_{kn}^{-1}(\vec{Q}_\perp)$ are eventually determined by the temperature dependent local orientational and positional order profiles in the film (see Sec. II).

Thus the relations obtained allow to calculate the specular and diffuse x-ray reflectivities of FSS*A*F in a self-consistent way and with taking into account its inhomogeneous and temperature dependent structure.

IV. RESULTS OF NUMERICAL CALCULATIONS AND DISCUSSION

A. Smectic layer displacement fluctuations and correlations between them

Numerical calculations of the smectic layer displacement fluctuations σ_n and correlations $g_{k,n}(R)$ have been carried out for two FSS*A*F's consisting of $N=24$ smectic layers. The first film is assumed to be created of LC exhibiting a ''strong'' first order Sm*A*-*I* phase transition. According to the McMillan theory [43] for the bulk Sm*A* phase and the microscopic model for FSS*A*F's proposed in Refs. [35,36] and [39], in this case the model parameter $\alpha=2\exp[-(\pi r_0/d)^2]$ used in the theory must be $\alpha\geqslant 0.98$. Here r_0 is a characteristic radius of the model pair potential proposed by McMillan. In our calculations we used $\alpha=1.05$. The second FSS*A*F is assumed to be made of LC having a ''weak'' first order Sm*A*-*N* phase transition. This case corresponds to $\alpha\leqslant 0.98$ [43]. Our calculations have been performed for $\alpha=0.871$. Our choice of values of the model parameter α is caused by that the LC compounds exhibiting such bulk phase transitions were used in experiments [18,26–28] on the small angle x-ray scattering from FSS*A*F's. In Refs. [26,27] the objects of study are FSS*A*F's made of the compound 4-heptyl-2-[4-(2-perfluorhexylethyl)phenyl]-pyrimidin (FPP) having the ''strong'' first order Sm*A*-*I* phase transition, whereas in Refs. [18] and [28] the thermal fluctuations and correlations between them are investigated in FSS*A*F's of LC 4, 4'-diheptylazoxybenzene (7AB) with the weak first order Sm*A*-*N* phase transition. In both cases, the smectic layer displacement fluctuations in FSS*A*F and the correlations between them have been calculated for two temperatures. The first temperature, $T_1^{(1,2)}$, is well below the bulk Sm*A*-*I* (Sm*A*-*N*) transition point, and the second one, $T_2^{(1,2)}$, is just below the maximum temperature at which FSS*A*F of given thickness ($N=24$) exists. For the first film, the temperature $T_1^{(1)}$ has been chosen $T_1^{(1)}=0.205(V_0/k_B)$, and $T_2^{(1)}=0.2298(V_0/k_B)$. Here V_0 is the intermolecular interaction constant in the McMillan theory [43]. According to this theory, for $\alpha=1.05$, the bulk Sm*A*-*I* transition temperature is equal to $T_{AI}=0.2249(V_0/k_B)$. On the other hand, according to the model [35,36,39] for FSS*A*F's, for $\alpha=1.05$, the maximum temperature of existence of the 24-layer film is equal to $T_c^{(1)}(N=24)=0.2299(V_0/k_B)$. Above this temperature the film either ruptures or undergoes the layer-thinning transition. For second FSS*A*F ($\alpha=0.871$), the first temperature $T_1^{(2)}$ has been taken $T_1^{(2)}=0.204(V_0/k_B)$ [according to the McMillan theory [43], for $\alpha=0.871$ the bulk Sm*A*-*N* transition temperature T_{AN} is equal to $T_{AN}=0.2091(V_0/k_B)$], and the second one is equal to $T_2^{(2)}=0.210\,35(V_0/k_B)$ [according to the model [35,36,39], for $\alpha=0.871$, the maximum temperature of existence of the 24-layer FSS*A*F is equal to $T_c^{(2)}(N=24)=0.210\,36(V_0/k_B)$]. For the first film, the magnitude of the intermolecular interaction constant V_0 has been chosen to provide a coincidence between the absolute bulk Sm*A*-*I* phase transition temperature T_{AI} given by theory and the experimentally found one (396 K [26,27]) in the LC compound FPP. Similarly, the magnitude of V_0 for second FSS*A*F has been chosen to provide a coincidence between theoretical value T_{AN} of the absolute bulk Sm*A*-*N* phase transition temperature with corresponding value (326 K [18,28]) experimentally found for LC 7AB. An orienting action of the boundary free surfaces of both films on the LC molecules has been assumed to be strong enough. The ratio W/V_0, where W is the interaction constant, which, in the framework of the model [35,36,39], determines the strength of the ''effective field'' simulating this action, has been set $W/V_0=1.6$. According to the model, for such sufficiently strong orienting action of the boundary free surfaces of FSS*A*F on the LC molecules, the N-layer film does not rapture upon heating above the maximum temperature $T_c(N)$, but undergoes the layer thinning transition. Just the same phenomena were observed in experiments [18,28] on FSS*A*F's of the compound 7AB. As for LC FPP investigated in Refs. [26] and [27], it is composed of the molecules having the partially perfluorinated alkyl tails. According to Refs. [14] and [16], FSS*A*F's of such LC's also do not rupture upon heating above $T_c(N)$ and exhibit the layer-thinning transitions.

For both FSS*A*F's, the bending elastic constant K_0 for the bulk Sm*A* phase at the temperature T_0 well below T_{AI} or T_{AN} (for LC with the bulk Sm*A*-*I* phase transition, we set $T_0=T_1^{(1)}$, and for LC having the bulk Sm*A*-*N* transition $T_0=T_1^{(2)}$) has been assumed to be $K_0=10^{-6}$ dyn (typical value for most LC's [40,41]). Similarly, the smectic layer compressibility B_0 for the bulk Sm*A* phase at the temperature T_0 has been assumed to be determined at the temperatures $T_1^{(1)}$ and $T_1^{(2)}$ for the first and second FSS*A*F, respectively. As for the absolute value of this elastic constant, for the first film we use the value found in Refs. [26] and [27] ($B_0=7.5\times10^9$ dyn/cm^2), and for the second one the value determined in Ref. [28] ($B_0=10^8$ dyn/cm^2). Values of the surface tensions γ of the FSS*A*F's, namely, $\gamma=13$ dyn/cm for the first film, and $\gamma=25$ dyn/cm for the second FSS*A*F, have been also taken from Refs. [18] and [26]–[28]. The film layer spacing d is assumed to be temperature independent and equal to $d=30$ A, and we set the molecular diameter $a=4$ A (typical value for the LC molecules [40,41]).

First of all, using the model [35,36,39], for both FSS*A*F's we have calculated the bending elastic constant K and the smectic layer compressibility B profiles. For the first film these profiles are shown in Figs. 1 and 2, respectively. From these figures it is seen (curves 1) that well below the bulk Sm*A*-*I* transition temperature ($T=T_1^{(1)}$), both elastic constants are similar for all film layers, with the exception of the outermost ones. In this case FSS*A*F is really spatially homogeneous, or nearly homogeneous, and the Holyst model [31,32] should give results similar to ours. However, close to the maximum temperature of existence of the 24-layer FSS*A*F ($T=T_2^{(1)}$), the film is no longer spatially uniform (curves 2), and the elastic constants K and B in its interior are significantly smaller than near the boundary free surfaces. In addition, Fig. 2 demonstrates the heating-induced decrease of the smectic layer compressibility B at the free surfaces as

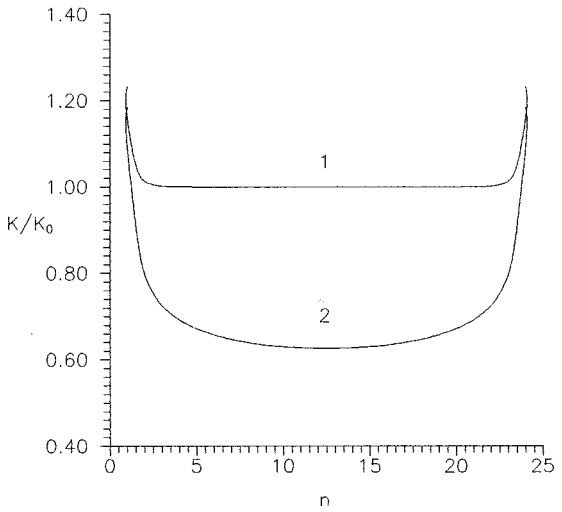

FIG. 1. The bending elastic constant K profiles (in dimensionless units) in the first FSSAF well below the bulk SmA-I transition temperature and near the maximum temperature of existence of the film. n is the film layer index. $N=24$; $\alpha=1.05$; $W/V_0=1.6$. 1: $T=T_1^{(1)}=0.205(V_0/k_B)$; 2: $T=T_2^{(1)}=0.2298(V_0/k_B)$.

well as in the interior film layers. Consequently, just in this case, a difference between predictions of the Holyst model [31,32] and our results should be noticeable. It should be noted that the elastic constant profiles for the second FSSAF, which are not shown here, are analogous to those depicted in Figs. 1 and 2.

Further, the elastic constant profiles obtained above have been used in calculations of the layer displacement fluctuation profiles σ_n for both FSSAF's. The results of these calculations are shown in Figs. 3 and 4, respectively. In the same figures, using the dashed curves, the thermal fluctuation profiles obtained in the framework of the Holyst model are also shown. As expected, for both films, our results obtained well below the bulk SmA-I ($T=T_1^{(1)}$) and SmA-N ($T=T_1^{(2)}$) phase transition temperatures are very similar to

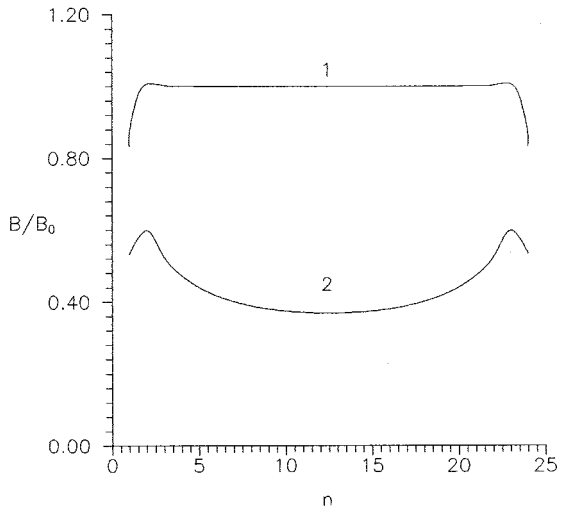

FIG. 2. The smectic layer compressibility B profiles in the first FSSAF under the same conditions as in Fig. 1. 1: $T=T_1^{(1)}=0.205(V_0/k_B)$; 2: $T=T_2^{(1)}=0.2298(V_0/k_B)$.

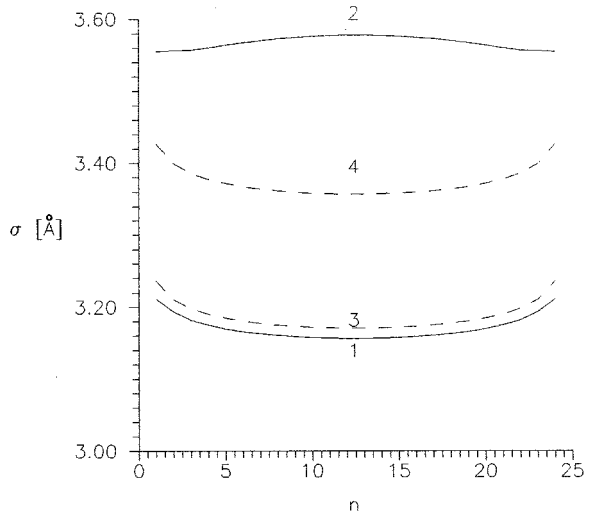

FIG. 3. The smectic layer displacement fluctuation profiles in the first FSSAF. $K_0=10^{-6}$ dyn; $B_0=7.5\cdot10^9$ dyn/cm^2; $\gamma=13$ dyn/cm. Other parameters are the same as in Figs. 1 and 2. The dashed curves represent the results of the Holyst model [31,32]. 1: $T=T_1^{(1)}=0.205(V_0/k_B)$; 2: $T=T_2^{(1)}=0.2298(V_0/k_B)$; 3: the result of the Holyst model at $T=T_1^{(1)}$; 4: the result of the same model at $T=T_2^{(1)}$.

those given by this model (in Fig. 4 the profile σ_n obtained at $T=T_1^{(2)}$ from the model [31,32] is not shown, because it coincides completely with our profile). However, for both FSSAF's, close to the maximum temperatures of their existence ($T=T_2^{(1,2)}$), the dependence of the elastic constants K and B on a distance from the boundary free surfaces of the films gives rise to a considerable deviation from the Holyst model [31,32] predictions. So, for the first FSSAF, (see Fig. 3), the difference between the σ_n profiles calculated at $T=T_1^{(1)}$ and $T=T_2^{(1)}$, respectively, with taking into account

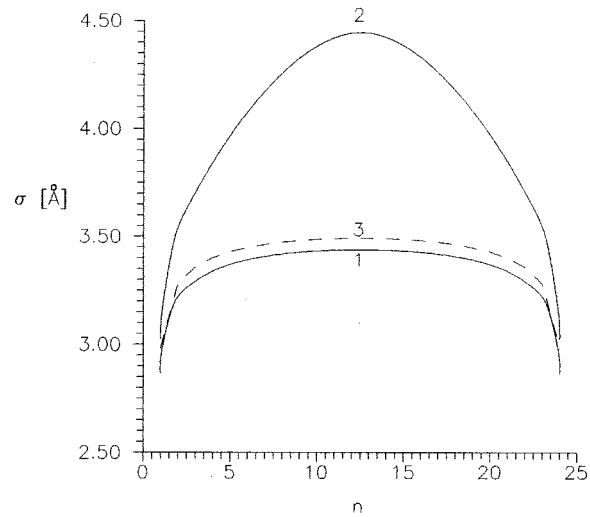

FIG. 4. The smectic layer displacement fluctuation profiles in the second FSSAF. $N=24$; $\alpha=0.871$; $W/V_0=1.6$; $K_0=10^{-6}$ dyn; $B_0=10^8$ dyn/cm^2; $\gamma=25$ dyn/cm. The dashed curve represents the results of the Holyst model [31,32]. 1: $T=T_1^{(2)}=0.204(V_0/k_B)$; 2: $T=T_2^{(2)}=0.210\,35(V_0/k_B)$; 3: the result of the Holyst model at $T=T_2^{(2)}$.

the elastic constant profiles shown in Figs. 1 and 2, is about two times larger than that given by the Holyst model. In addition, according to Refs. [31] and [32], the growth of temperature only increases the average amplitudes σ_n of the thermal fluctuations in the film and does not change the shape of the fluctuation profile which has maximum at the boundary free surfaces of the film and minimum in its interior (see Fig. 3, curves 3 and 4). On contrary, our calculation, which takes into account the temperature dependences of the elastic constant profiles, shows that heating the film to the maximum temperature of its existence not only gives rise to the growth of the absolute value of σ_n, but also changes the shape of the smectic layer displacement fluctuation profile (see Fig. 3, curves 1 and 2). It is clear that for $T=T_2^{(1)}$ the value of σ_n in interior of the film becomes larger than near the boundary free surfaces of FSS*A*F. As for the second FSS*A*F, close to the maximum temperature of its existence ($T=T_2^{(2)}$), the difference between our results and those given by the Holyst model is much more pronounced than for the first film. As in previous case, this model predicts a very weak change in the thermal fluctuation profile σ_n upon increasing temperature of the film (Fig. 4, curve 3), whereas our calculation gives quite different result (Fig. 4, curve 2). First, for $T=T_2^{(2)}$, the absolute value σ_n of the layer displacement fluctuations in interior of the film is about 30% larger than for $T=T_1^{(2)}$. Second, the initially flat enough fluctuation profile becomes ''domelike'' at $T=T_2^{(2)}$. It should be noticed that similar changes in the fluctuation profiles with increasing temperature of the film have been obtained in experiments [18] and [28] on the small angle x-ray scattering from FSS*A*F's made of the compound 7AB (analogous experiments [26,27] on FSS*A*F's of the LC FPP have been performed only well below the bulk Sm*A*-*I* transition temperature). Thus our theoretical results are in a better agreement with experiments [18,28] than predictions of the Holyst model [31,32].

We have also calculated the correlations $g_{k,n}(R)$ between the displacement fluctuations of different layers in FSS*A*F's. The results of these calculations for correlations between the fluctuations of the first film layer ($k=1$) and other layers ($n=1,24,\vec{R}=0$) for the first and second films are shown in Fig. 5 and 6, respectively. In both cases, well below the bulk Sm*A*-*I* or Sm*A*-*N* transition temperatures ($T=T_1^{(1,2)}$), our results (curves 1 in Figs. 5 and 6) are completely similar to those predicted by the Holyst model [31,32] (dashed curves in these figures). However, for the maximum temperatures ($T=T_2^{(1,2)}$) of existence of both FSS*A*F's, our values of the correlations $g_{1,n}(0)$ (curves 2 in Figs. 5 and 6) are noticeably different from the correlations given by this model. According to the Holyst theory, the correlations $g_{k,n}(0)$ are practically insensitive to the growth of temperature of the film [in Figs. 5 and 6, for $T=T_2^{(1,2)}$, the correlations $g_{1,n}(0)$ are given by the same dashed curves as for $T=T_1^{(1,2)}$]. On contrary, our calculations show that increasing the temperature does not affect only correlations between the fluctuations of neighboring smectic layers. When the kth and nth layers are disposed sufficiently far from each other, the correlations $g_{k,n}(0)$ decrease with increasing temperature, and a largest decay occurs for correlation between the fluctuations of the first and last film layers. For example, in the first FSS*A*F (see

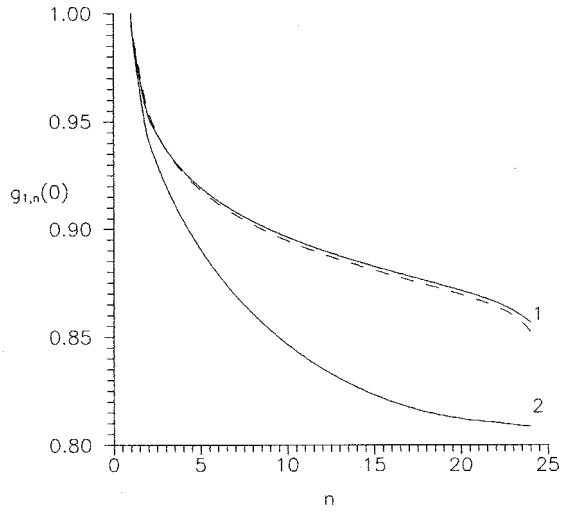

FIG. 5. The correlations $g_{1,n}(0)$ between the displacement fluctuations of the first and other smectic layers ($n=1,24$) in the first FSS*A*F. The curves 1 and 2 represent the results of our calculations for $T=T_1^{(1)}=0.205(V_0/k_B)$ and $T=T_2^{(1)}=0.2298(V_0/k_B)$, respectively. The dashed curve represents the results of the Holyst model.

Fig. 5) the correlation $g_{1,24}(0)$ at $T=T_2^{(1)}$ is about 6% smaller than at the initial temperature $T=T_1^{(1)}$, and for the second FSS*A*F, the growth of temperature from $T=T_1^{(2)}$ to $T=T_2^{(2)}$ gives rise to about 34% decay of $g_{1,24}(0)$. Such decay of the correlations $g_{1,24}(0)$ is due to a significant decrease of the elastic moduli K and B in interior of the films upon heating to the maximum temperatures $T=T_2^{(1,2)}$ of their existence (see Figs. 1 and 2) which is completely ignored in the Holyst model [31,32]. Since the smectic displacement fluctuations near the one boundary free surface of the film are connected with those near the second boundary free surface via the central region of the film, a weakening latter should give rise to the decay of correlations between these fluctuations.

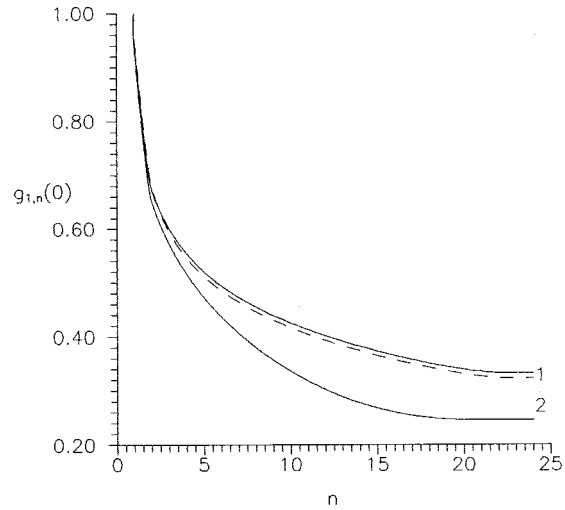

FIG. 6. The same correlations as in Fig. 5 but for the second FSS*A*F. The curves 1 and 2 correspond to the results of our calculations $T=T_1^{(2)}=0.204(V_0/k_B)$ and $T=T_2^{(2)}=0.210\,35(V_0/k_B)$, respectively. The dashed curve corresponds to the results of the Holyst model.

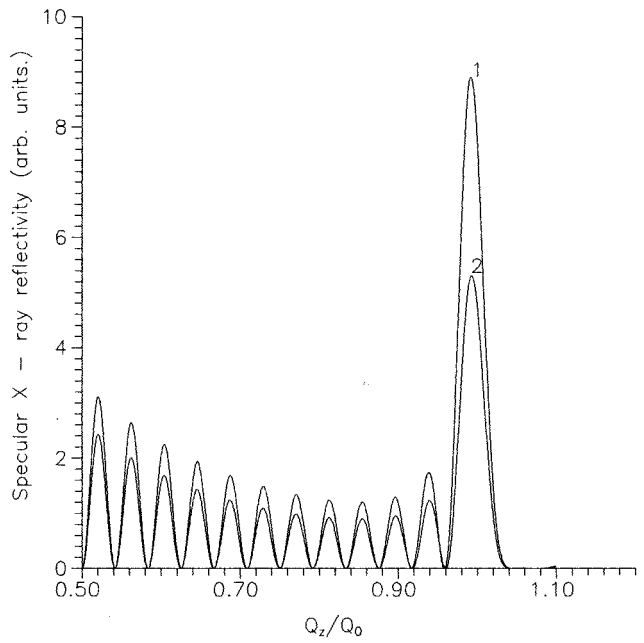

FIG. 7. Dependence of the specular x-ray reflectivity of the first FSS*A*F (in arbitrary units) on the component Q_z of the wave vector transfer. 1: $T=T_1^{(1)}=0.205(V_0/k_B)$; 2: $T=T_2^{(1)}=0.2298(V_0/k_B)$.

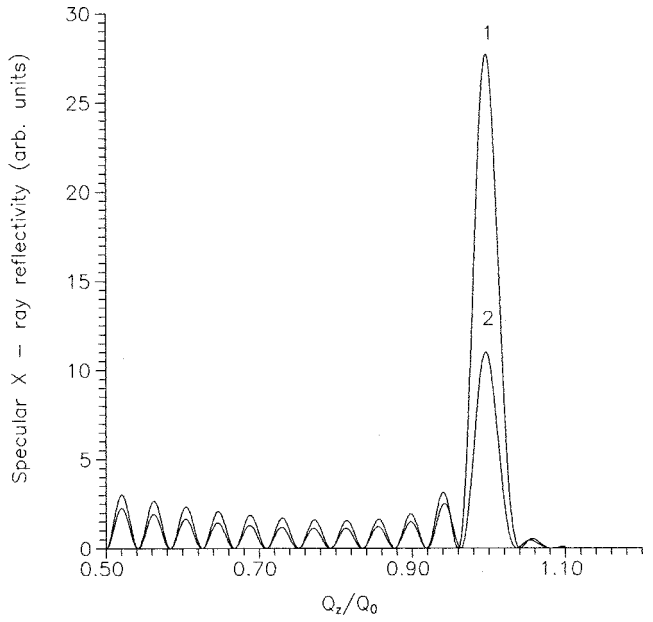

FIG. 8. The similar dependence for the second FSS*A*F. $T=T_1^{(2)}=0.204(V_0/k_B)$ and $T=T_2^{(2)}=0.210\,35(V_0/k_B)$.

B. Specular and diffuse x-ray reflectivities of FSS*A*F

The results obtained above have been used in computation of the specular and diffuse x-ray reflectivities of 24-layer FSS*A*F's having the bulk Sm*A*-*I* and Sm-*N* phase transitions. As in Refs. [18] and [26–28], we use expression (26) for the molecular form factor and set the molecular length $L=29$ A. We also use $(\rho_{tail}/\rho_{core})=1.14$, and $d_{tail}=0.29L$ for the first FSS*A*F [26,27], and $(\rho_{tail}/\rho_{core})=1/1.5$, and $d_{tail}=0.23L$ for the second one [18,28].

The dependences of the specular x-ray reflectivities (in arbitrary units) of both FSS*A*F's on the component Q_z of the wave vector transfer are shown in Figs. 7 and 8. In these figures, the curves 1 correspond to the temperatures $T=T_1^{(1)}$ and $T=T_1^{(2)}$ which are we well below the bulk Sm*A*-*I* and Sm*A*-*N* phase transition points, respectively, and curves 2 demonstrate analogous dependences for maximum temperatures $T=T_2^{(1)}$ and $T=T_2^{(2)}$ of existence of the films. All curves in Figs. 7 and 8 have the primary (first) Bragg peaks at $Q_z=Q_0=2\pi/d$, which are due to a constructive interference of x rays reflected from all film layers. These curves also exhibit a series of secondary oscillations (the Kiessig fringes) which are caused by constructive and destructive interference of x rays reflected from the boundary surfaces of the films [26–28]. It is clearly seen that, for both FSS*A*F's, the growth of temperature gives rise to a small change in intensities of the Kiessig fringes, whereas, for the first film, the first Bragg peak at the maximum temperature $T=T_2^{(1)}$ is about 40% lower than that at $T=T_1^{(1)}$ (see Fig. 7), and, for the second FSS*A*F, the first Bragg peak becomes about 2.5 times lower with increasing temperature from $T=T_1^{(2)}$ to $T=T_2^{(2)}$ (see Fig. 8). Just the same behavior has been observed in experiments on the small angle x-ray scattering from FSS*A*F's made of the compound 7AB [18,28]. Although analogous experiments on the free-standing films of LC FPP [26,27] have been made only well below the bulk Sm*A*-*I* phase transition temperature, and therefore now it is impossible to compare the results demonstrated in Fig. 7 with experiment, we believe that such films should exhibit a similar behavior upon heating well above the bulk Sm*A*-*I* transition point.

The results obtained can be physically interpreted as follows. The microscopic model [35,36,39] for FSS*A*F's, which is used in our calculations of the coefficients η_k, the amplitudes σ_k of the smectic layer displacement fluctuations, and correlations between them, predicts an insignificant enough weakening both the orientational and positional order within the outermost film layers upon heating above the bulk Sm*A*-*I* or Sm*A*-*N* transition temperature. At the same time, according to this model, near the maximum temperature of existence of the film ($T=T_2^{(1,2)}$), both the orientational and positional order in its interior layers should be much lower than well below the bulk Sm*A*-*I* or Sm*A*-*N* transition point. Since the interference between x rays reflected from the interior film layers contributes only to intensity of the Bragg peak, weakening the order in the interior of FSS*A*F gives rise to decay of this intensity and does not affect noticeably the intensities of the Kiessig fringes. So, the experimentally observed considerable decrease in the intensity of the first Bragg peak and sufficiently small change in intensities of the Kiessig fringes can be considered as conformation of the model for FSS*A*F's proposed in Refs. [35,36] and [39]. In addition, our theoretical results can be obtained without introducing some *ad hoc* values which, as said in the Introduction, are required to fit the Holyst model [31,32] to the experimental data [18,28].

The results of numerical calculation of the diffuse x-ray reflectivity of the second FSS*A*F for temperatures $T=T_1^{(2)}$ and $T=T_2^{(2)}$ are shown in Figs. 9 and 10, respectively (analogous results for the first film are qualitatively very similar and therefore are not shown here). These figures demonstrate dependences of the diffuse x-ray reflectivity of FSS*A*F (in

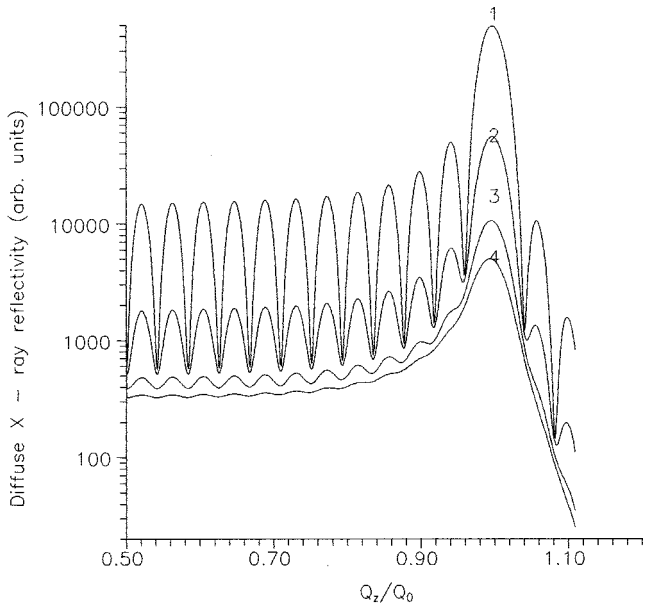

FIG. 9. The Q_z dependence of the diffuse x-ray reflectivity of the second FSS*A*F (in arbitrary units) for different values of the transverse component $Q_\perp$ of the wave vector transfer. $T=T_1^{(2)}=0.204(V_0/k_B)$. 1: $Q_\perp/Q_1=0.001$; 2: $Q_\perp/Q_1=0.003$; 3: $Q_\perp/Q_1=0.007$; 4: $Q_\perp/Q_1=0.01$.

arbitrary units) on the component Q_z of the wave vector transfer for several values of its transverse component $Q_\perp$. Similarly to the specular reflectivity of FSS*A*F (see Figs. 7 and 8), these dependences demonstrate the first Bragg peaks at $Q_z=Q_0=2\pi/d$, which are due to a constructive interference of x rays scattered from all film layers, and a series of the Kiessig fringes which are caused by constructive and destructive interference of x rays scattered from the boundary surfaces of the film. In Refs. [18] and [26]–[28] it has been pointed out that occurrence of these maxima and minima in the x-ray diffuse scattering patterns can be considered as an evidence of a conformality of the smectic layer displacement fluctuations in FSS*A*F. In other words, the thermal fluctuations in the film are not independent of each other, and different film layers fluctuate ''in unison.'' It is also seen that maxima of the x-ray diffuse reflectivity decrease with increasing the transverse component $Q_\perp$ of the wave vector transfer, and decay of the secondary maxima is faster than that of the first Bragg peak. Eventually, for a certain value of $Q_\perp$, the Kiessig fringes become completely suppressed, whereas the Bragg peak, though very wakened and smoothed, is still observed. Thus one can conclude that the smectic layer displacement fluctuations lose their conformality with growth of $Q_\perp$, i.e., with decreasing wavelength of the displacement undulation modes [18,26–28]. Moreover, the faster decay of the Kiessig fringes suggests that the fluctuations of the outermost film layers, which are disposed at a longest distance from each other, lose the conformality earlier than fluctuations of other film layers.

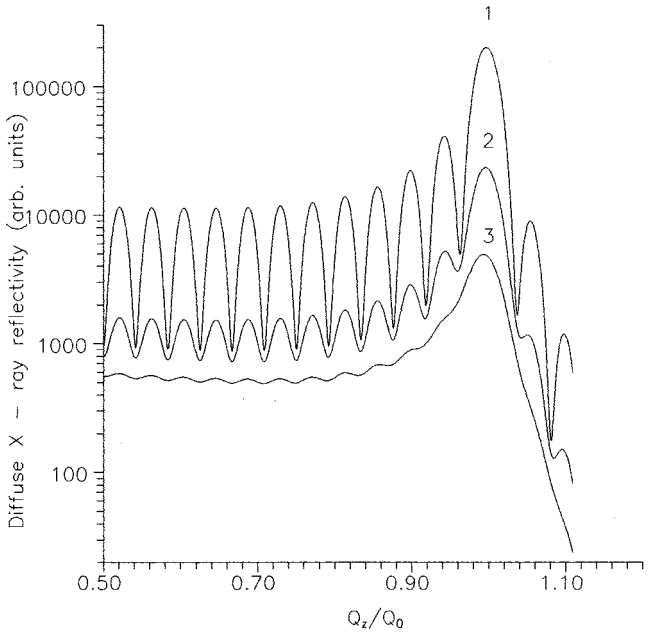

FIG. 10. The analogous dependence for $T=T_2^{(2)}=0.210\,35(V_0/k_B)$. 1: $Q_\perp/Q_1=0.001$; 2: $Q_\perp/Q_1=0.003$; 3: $Q_\perp/Q_1=0.007$.

These results, which are in a good agreement with experiment [18,28,29], can be also obtained in the frame work of the Holyst model [32,32]. However, Figs. 9 and 10 demonstrate one very essential feature of behavior of the diffuse x-ray reflectivity of FSS*A*F which cannot, in principle, be obtained from the Holyst theory and its continuous extensions [33,34]. One can conclude from these figures that, near the maximum temperature of existence of the film ($T=T_2^{(2)}$), the smectic layer displacement fluctuations must lose conformality with growth of $Q_\perp$ earlier than it occurs at lower temperature $T=T_1^{(2)}$. So, according to Fig. 9 ($T=T_1^{(2)}$), for $Q_\perp=0.007Q_1$, where $Q_1=2\pi/a$, the Kiessig fringes, though very weak, are still observed. At the same time, one can see in Fig. 10 that, for $T=T_2^{(2)}$, the Kiessig fringes are almost completely suppressed at the same value of $Q_\perp$. It means that near the maximum temperature of existence of FSS*A*F the thermal fluctuations of the outermost film layers become independent of each other for lower values of $Q_\perp$, i.e., for longer wavelengths of the displacement undulation modes, than it occurs at lower temperatures of the film. According to Eq. (28), intensity of the diffuse x-ray scattering from FSS*A*F is proportional to correlations between the thermal fluctuations of different film layers. As said above (see Figs. 5 and 6), the growth of temperature of the film gives rise to weakening these correlations, and this weakening is most pronounced for the correlations between fluctuations of the outermost film layers. Such a decay of the correlation is due to the significant decrease of the elastic moduli *K* and *B* in the interior of the film which is ignored in the Holyst theory [31,32]. Unfortunately, in Refs. [18,28] the diffuse x-ray scattering from FSS*A*F's has been studied only well below the bulk Sm*A*-*N* transition temperature, and now we cannot compare our theoretical results with experiment. Therefore the experimental investigation of the diffuse x-ray reflectivity of FSS*A*F's near the maximum temperature of their existence seems to be very interesting.

ACKNOWLEDGMENT

This work was supported by the Russian Fund of Fundamental Investigations (Grant No. 98-03-32448).

[1] P. Pieranski, L. Beliard, J. P. Tournellec, X. Leoncini, C. Furtlehner, H. Dumoulin, E. Riou, B. Jouvin, J. P. Fenerol, Ph. Palaric, J. Heuving, B. Cartier, and I. Kraus, Physica A **194**, 364 (1993).
[2] C. Rosenblatt, R. Pindak, N. A. Clark, and R. B. Meyer, Phys. Rev. Lett. **42**, 1220 (1979).
[3] M. Veum, C. C. Huang, C. F. Chou, and V. Surendranath, Phys. Rev. E **56**, 2298 (1997).
[4] C. Rosenblatt and N. M. Amer, Appl. Phys. Lett. **36**, 432 (1980).
[5] S. Heinekamp, R. A. Pelcovits, E. Fontes, E. Y. Chen, R. Pindak, and R. B. Meyer, Phys. Rev. Lett. **52**, 1017 (1984).
[6] R. Pindak, D. J. Bishop, and W. O. Sprenger, Phys. Rev. Lett. **44**, 1461 (1980).
[7] J. C. Tarczon and K. Miyano, Phys. Rev. Lett. **46**, 119 (1981).
[8] D. J. Bishop, W. O. Sprenger, R. Pindak, and M. E. Neubert, Phys. Rev. Lett. **49**, 1861 (1982).
[9] C. Bahr and D. Fliegner, Phys. Rev. A **46**, 7657 (1992).
[10] I. Kraus, P. Pieranski, E. Demikhov, H. Stegemeyer, and J. Goodby, Phys. Rev. E **48**, 1916 (1993).
[11] J. Collet, P. S. Pershan, E. B. Sirota, and L. B. Sorensen, Phys. Rev. Lett. **52**, 356 (1984).
[12] E. B. Sirota, P. S. Pershan, L. B. Sorensen, and J. Collet, Phys. Rev. Lett. **55**, 2039 (1985).
[13] E. B. Sirota, P. S. Pershan, L. B. Sorensen, and J. Collet, Phys. Rev. A **36**, 2890 (1987).
[14] T. Stoebe, P. Mach, and C. C. Huang, Phys. Rev. Lett. **73**, 1384 (1994).
[15] E. I. Demikhov, V. K. Dolganov, and K. P. Meletov, Phys. Rev. E **52**, R1285 (1995).
[16] V. K. Dolganov, E. I. Demikhov, R. Fouret, and C. Gors, Phys. Lett. A **220**, 242 (1996).
[17] P. Johnson, P. Mach, E. D. Wedell, F. Lintgen, M. Neubert, and C. C. Huang, Phys. Rev. E **55**, 4386 (1997).
[18] E. A. L. Mol, G. C. L. Wong, J. M. Petit, F. Rieutord, and W. H. de Jeu, Physica B **248**, 191 (1998).
[19] C. Y. Young, R. Pindak, N. A. Clark, and R. B. Meyer, Phys. Rev. Lett. **40**, 773 (1978).
[20] R. Geer, C. C. Huang, R. Pindak, and J. W. Goodby, Phys. Rev. Lett. **63**, 540 (1989).
[21] P. Mach, S. Grantz, D. A. Debe, T. Stoebe, and C. C. Huang, J. Phys. II **5**, 217 (1995).
[22] J. D. Brock, R. J. Birgeneau, J. D. Litster, and A. Aharony, Contemp. Phys. **30**, 321 (1989).
[23] S. Amador, P. S. Pershan, H. Stragier, B. D. Swanson, D. J. Tweet, L. B. Sorensen, E. B. Sirota, G. E. Ice, and A. Habenschuss, Phys. Rev. A **39**, 2703 (1989).
[24] E. B. Sirota, P. S. Pershan, S. Amador, L. B. Sorensen, Phys. Rev. A **35**, 2283 (1987).
[25] P. Lambooy, S. Gierlotka, and W. H. de Jeu, Europhys. Lett. **12**, 341 (1990).
[26] J. D. Shindler, E. A. L. Mol, and A. Shalaginov, Phys. Rev. Lett. **74**, 722 (1995).
[27] J. D. Shindler, E. A. L. Mol, A. Shalaginov, and W. H. de Jeu, Phys. Rev. E **54**, 536 (1996).
[28] E. A. L. Mol, G. C. L. Wong, J. M. Petit, F. Rieutord, and W. H. de Jeu, Phys. Rev. Lett. **78**, 3157 (1997).
[29] C. Rosenblatt and D. Ronis, Phys. Rev. A **23**, 305 (1981).
[30] J. V. Selinger and D. R. Nelson, Phys. Rev. Lett. **61**, 416 (1988).
[31] R. Holyst and D. J. Tweet, Phys. Rev. Lett. **65**, 2153 (1990).
[32] R. Holyst, Phys. Rev. A **44**, 3692 (1991).
[33] A. Poniewerski and R. Holyst, Phys. Rev. B **47**, 9840 (1993).
[34] A. N. Shalaginov and V. P. Romanov, Phys. Rev. E **48**, 1073 (1993).
[35] L. V. Mirantsev, Phys. Lett. A **205**, 412 (1995).
[36] L. V. Mirantsev, Liq. Cryst. **20**, 417 (1996).
[37] T. Krancj and S. Zumer, J. Chem. Phys. **105**, 5242 (1996).
[38] Y. Martinez-Raton, A. M. Somoza, L. Mederos, and D. E. Sullivan, Phys. Rev. E **55**, 2030 (1997).
[39] L. V. Mirantsev, Phys. Rev. E **55**, 4816 (1997).
[40] P. G. de Gennes, *The Physics of Liquid Crystals* (Clarendon, Oxford, 1974).
[41] S. Chandrasekhar, *Liquid Crystals* (Cambridge University Press, Cambridge, 1977).
[42] L. V. Mirantsev, Liq. Cryst. (to be published).
[43] W. L. McMillan, Phys. Rev. A **4**, 1238 (1971).